Physica B 705 (2025) 417095

Contents lists available at ScienceDirect

Physica B: Condensed Matter

journal homepage: www.elsevier.com/locate/physb

Comprehensive analysis of structural, optical, and photocatalytic properties of single-phase calcium vanadates: Insights into CaV_2O_6 and $Ca_2V_2O_7$

N. Abhiram [a,b], Bagavathy Shunmughananthan [a,c], Ajay Kesavan [d], Mohammed Mujahid Alam [e,f,**], Abdullah G. Al-Sehemi [e,f], Thangaraju Dheivasigamani [a,*]

[a] Nano-crystal Design and Application Lab (n-DAL), Department of Physics, PSG Institute of Technology and Applied Research, Coimbatore, 641062, Tamil Nadu, India
[b] Department of Physics, Dhanekula Institute of Engineering & Technology, Ganguru, Vijayawada, 521139, Andhra Pradesh, India
[c] Centre for Advanced Materials, PSG College of Arts & Science, Coimbatore - 641014, Tamil Nadu, India
[d] Department of Mechanical Engineering, PSG Institute of Technology and Applied Research, Coimbatore, 641062, Tamil Nadu, India
[e] Central Labs, King Khalid University, AlQura'a, P.O. Box 960, Abha, Saudi Arabia
[f] Department of Chemistry, College of Science, King Khalid University, Abha, 61413, Saudi Arabia

ARTICLE INFO

Keywords:
Photocatalyst
Dye degradation
Methylene blue
Calcium vanadates

ABSTRACT

The primary issue related to industrialization is that environmental pollution contributes to human health hazards. One significant cause of environmental contamination is the usage of various dyes in industries. In this context, photocatalysis plays a significant role due to its inherent nature. The cost-effective gel matrix method synthesized two distinct phases of calcium vanadate. The prepared vanadates' phase formation, crystallinity, optical properties and elemental composition were investigated using X-ray Diffraction (XRD), Raman spectroscopy, UV–visible spectroscopy and X-ray Photoelectron Spectroscopy (XPS). The band gap calculation was done from the Tauc plot using the UV absorbance studies. The morphology of the synthesized vanadates was examined using Scanning Electron Microscopy (SEM). Employing methylene blue (MB) as a model dye, the dye degradation illustrated the photocatalytic activity of synthesized semiconductor photocatalyst by irradiating visible light. The degradation efficiency of $Ca_2V_2O_7$ is 97 % within 4 h, which can be used for removing the dyes from the waste waters.

1. Introduction

The worldwide water resources have been heavily exploited due to the development of various industries and rapid population growth. Serious ecological and environmental problems arise from the untreated release of wastewater from industries which release hazardous dye compounds into river streams and lakes. Numerous water treatment approaches following chemical, physical or biological processes have been developed to address this problem [1]. The conventionally used techniques merely transfer pollutants to a different phase or produce secondary pollutants, necessitating additional treatment and having an expensive and time-consuming operating process [2]. Recently, the advanced oxidation process (AOP) has emerged as a viable technology for treating contaminants in water [3]. Typically, AOP employs extremely active species that initiate a chain of events that convert contaminants into harmless compounds. Photocatalysis, an advanced oxidation process, has garnered significant interest in water purification due to its easy operating parameters, environmental friendliness, lack of waste byproducts, and complete degradation [4,5]. It is a sustainable process with ease and efficacy that can effectively eliminate/degrade harmful compounds from pollutant water [6–9], including organic pollutants such as rhodamine B, methyl red, congo red, methylene blue, methyl orange, and others from dye effluent [10–12]. Photocatalysts with specific morphologies have enormous applications for degrading hazardous contaminants from industrial effluent [13]. The desired photocatalysts should have excellent crystallinity, ease of handling, relatively inexpensive, non-toxicity, large surface area, low-cost application, and not release noxious or fatal by-products [14]. Photocatalysts with thermal/photochemical stability, best band gap, recyclability, and catalytic activity are required to degrade the dyes or contaminants [15]. The advanced oxidation process (AOP), which uses semiconductor photocatalysts to remove natural contaminants from wastewater, has

* Corresponding author.
** Corresponding author. Central Labs, King Khalid University, AlQura'a, P.O. Box 960, Abha, Saudi Arabia.
E-mail addresses: malm@kku.edu.sa (M.M. Alam), dthangaraju@gmail.com (T. Dheivasigamani).

https://doi.org/10.1016/j.physb.2025.417095
Received 23 December 2024; Received in revised form 21 February 2025; Accepted 28 February 2025
Available online 28 February 2025

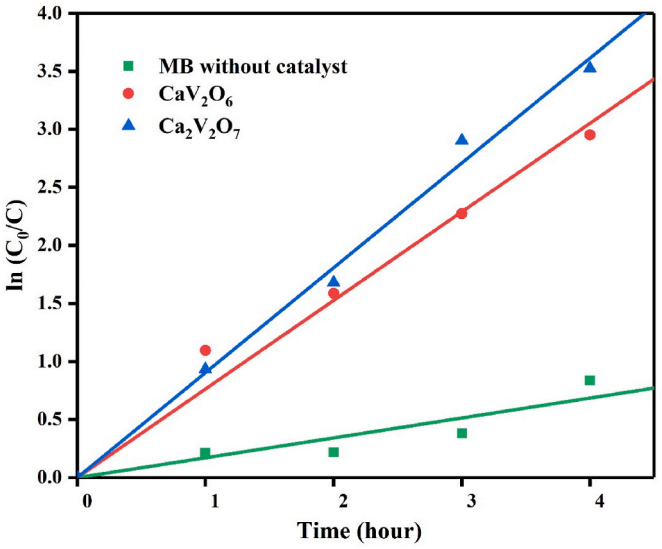

Fig. 9. Degradation kinetics of CaV_2O_6 and $Ca_2V_2O_7$ toward the removal of methylene blue: ln(C_0/C) vs. time. (For interpretation of the references to colour in this figure legend, the reader is referred to the Web version of this article.)

$$ln\left(\frac{C_0}{C}\right) = kt \tag{12}$$

Where C denotes the intensity of the absorption peak of Methylene blue samples at a specific time t (mg L^{-1}), C_0 is the intensity of the absorption peak of samples at initial time t_0 (mg L^{-1}), k is the rate constant (min^{-1}) and t is the light irradiated time (min) [45]. Fig. 9 represents the kinetic plot between the logarithm of the concentration ratio (ln (C_0/C)) and irradiation time (t). A linear, continuous line was observed for the degradation of MB dye with an R^2 value of 0.993 and 0.997 for CaV_2O_6 and $Ca_2V_2O_7$, respectively, indicating that the degradation reaction follows pseudo-first order kinetics as the correlation constant $R^2 > 0.95$. The degradation rates of the reaction corresponding to CaV_2O_6 and $Ca_2V_2O_7$ were found to be 0.7631 h^{-1} and 0.9035 h^{-1}, respectively. The result also indicates that with a higher rate of degradation, $Ca_2V_2O_7$ has degraded the dye effectively, which agrees with the corresponding degradation efficiency results.

4. Conclusion

This study used a facile sol-gel method to synthesize two different phases of calcium vanadates (CaV_2O_6 and $Ca_2V_2O_7$). The monoclinic and triclinic crystal structure and the formation of the phases were confirmed using XRD analysis. The vibrational modes of the material and the optical properties were investigated using Raman and UV–visible analysis. XPS analysis affirms the presence of all elements, thereby confirming the particle formation. The rod structure of the synthesized calcium vanadate particles was confirmed using SEM analysis. Photocatalytic activity carried out to examine the degradation of dye using the prepared $Ca_2V_2O_7$ catalyst, shows degradation efficiency of about 97 % in 4 h than CaV_2O_6.

CRediT authorship contribution statement

N. Abhiram: Writing – review & editing, Writing – original draft, Formal analysis, Data curation. **Bagavathy Shunmughananthan:** Writing – review & editing, Writing – original draft, Methodology, Formal analysis, Data curation. **Ajay Kesavan:** Methodology, Data curation. **Mohammed Mujahid Alam:** Writing – review & editing, Funding acquisition. **Abdullah G. Al-Sehemi:** Writing – review & editing, Funding acquisition. **Thangaraju Dheivasigamani:** Writing – review & editing, Validation, Supervision, Project administration, Methodology, Investigation, Data curation, Conceptualization.

Declaration of competing interest

There is no conflict of interest; if accepted, the article will not be published elsewhere in the same form, in any language, without the publisher's written consent.

Acknowledgement

The authors extend their appreciation to University Higher Education Fund for funding this research work under Research Support Program for Central labs at King Khalid University through the project number CL/RP/4.

Data availability

Data will be made available on request.

References

[1] I. Karuppusamy, M.S. Samuel, E. Selvarajan, S. Shanmugam, P. Sahaya Murphin Kumar, K. Brindhadevi, A. Pugazhendhi, Ultrasound-assisted synthesis of mixed calcium magnesium oxide (CaMgO2) nanoflakes for photocatalytic degradation of methylene blue, J. Colloid Interface Sci. 584 (2021) 770–778, https://doi.org/10.1016/j.jcis.2020.09.112.
[2] O. Mekasuwandumrong, P. Pawinrat, P. Praserthdam, J. Panpranot, Effects of synthesis conditions and annealing post-treatment on the photocatalytic activities of ZnO nanoparticles in the degradation of methylene blue dye, Chem. Eng. J. 164 (2010) 77–84, https://doi.org/10.1016/j.cej.2010.08.027.
[3] Y. Deng, R. Zhao, Advanced oxidation processes (AOPs) in wastewater treatment, Curr. Pollut. Reports. 1 (2015) 167–176, https://doi.org/10.1007/s40726-015-0015-z.
[4] K.K. Jaiswal, S. Dutta, C.B. Pohrmen, R. Verma, A. Kumar, A.P. Ramaswamy, Biowaste chicken eggshell-derived calcium oxide for photocatalytic application in methylene blue dye degradation under natural sunlight irradiation, Inorg. Nano-Metal Chem. 51 (2021) 995–1004, https://doi.org/10.1080/24701556.2020.1813769.
[5] S. Mondal, M.E. De Anda Reyes, U. Pal, Plasmon induced enhanced photocatalytic activity of gold loaded hydroxyapatite nanoparticles for methylene blue degradation under visible light, RSC Adv. 7 (2017) 8633–8645, https://doi.org/10.1039/C6RA28640B.
[6] S.K. Khetan, T.J. Collins, Human pharmaceuticals in the aquatic environment: a challenge to green chemistry, Chem. Rev. 107 (2007) 2319–2364, https://doi.org/10.1021/cr020441w.
[7] N. Prakash, D. Thangaraju, R. Karthikeyan, M. Arivanandhan, Y. Shimura, Y. Hayakawa, UV-visible and near-infrared active NaGdF4:Yb:Er/Ag/TiO2 nanocomposite for enhanced photocatalytic applications, RSC Adv. 6 (2016) 80655–80665, https://doi.org/10.1039/c6ra10208e.
[8] R. Ameta, M.S. Solanki, S. Benjamin, S.C. Ameta, Photocatalysis. https://doi.org/10.1016/B978-0-12-810499-6.00006-1, 2018.
[9] M. Pelaez, N.T. Nolan, S.C. Pillai, M.K. Seery, P. Falaras, A.G. Kontos, P.S. M. Dunlop, J.W.J. Hamilton, J.A. Byrne, K. O'Shea, M.H. Entezari, D.D. Dionysiou, A review on the visible light active titanium dioxide photocatalysts for environmental applications, Appl. Catal. B Environ. 125 (2012) 331–349, https://doi.org/10.1016/j.apcatb.2012.05.036.
[10] W. Zhao, Z. Wei, L. Zhang, X. Wu, X. Wang, Cr doped SnS2 nanoflowers: preparation, characterization and photocatalytic decolorization, Mater. Sci. Semicond. Process. 88 (2018) 173–180, https://doi.org/10.1016/j.mssp.2018.08.011.
[11] H. Zangeneh, A.A.L. Zinatizadeh, M. Habibi, M. Akia, M. Hasnain Isa, Photocatalytic oxidation of organic dyes and pollutants in wastewater using different modified titanium dioxides: a comparative review, J. Ind. Eng. Chem. 26 (2015) 1–36, https://doi.org/10.1016/j.jiec.2014.10.043.
[12] X. Zhao, H. Yang, S. Li, Z. Cui, C. Zhang, Synthesis and theoretical study of large-sized Bi4Ti3O12 square nanosheets with high photocatalytic activity, Mater. Res. Bull. 107 (2018) 180–188, https://doi.org/10.1016/j.materresbull.2018.07.018.
[13] K. Mageshwari, S.S. Mali, R. Sathyamoorthy, P.S. Patil, Template-free synthesis of MgO nanoparticles for effective photocatalytic applications, Powder Technol. 249 (2013) 456–462, https://doi.org/10.1016/j.powtec.2013.09.016.
[14] P. Singh, P. Shandilya, P. Raizada, A. Sudhaik, A. Rahmani-Sani, A. Hosseini-Bandegharaei, Review on various strategies for enhancing photocatalytic activity of graphene based nanocomposites for water purification, Arab. J. Chem. 13 (2020) 3498–3520, https://doi.org/10.1016/j.arabjc.2018.12.001.
[15] V.V. Gawade, N.L. Gavade, H.M. Shinde, S.B. Babar, A.N. Kadam, K.M. Garadkar, Green synthesis of ZnO nanoparticles by using Calotropis procera leaves for the

photodegradation of methyl orange, J. Mater. Sci. Mater. Electron. 28 (2017) 14033–14039, https://doi.org/10.1007/s10854-017-7254-2.
[16] A. Inderyas, I.A. Bhatti, A. Ashar, M. Ashraf, A. Ghani, M. Yousaf, M. Mohsin, M. Ahmad, S. Rafique, N. Masood, M. Iqbal, Synthesis of immobilized ZnO over polyurethane and photocatalytic activity evaluation for the degradation of azo dye under UV and solar light irradiation, Mater. Res. Express 7 (2020) 025033, https://doi.org/10.1088/2053-1591/ab715f.
[17] K. Lü, G.X. Zhao, X.K. Wang, A brief review of graphene-based material synthesis and its application in environmental pollution management, Chin. Sci. Bull. 57 (2012) 1223–1234, https://doi.org/10.1007/s11434-012-4986-5.
[18] L. Fan, C. Luo, M. Sun, H. Qiu, X. Li, Synthesis of magnetic β-cyclodextrin-chitosan/graphene oxide as nanoadsorbent and its application in dye adsorption and removal, Colloids Surf. B Biointerfaces 103 (2013) 601–607, https://doi.org/10.1016/j.colsurfb.2012.11.023.
[19] J. Fan, T. Li, H. Heng, Hydrothermal growth of ZnO nanoflowers and their photocatalyst application, Bull. Mater. Sci. 39 (2016) 19–26, https://doi.org/10.1007/s12034-015-1145-z.
[20] W. Remlalfaka, C. Murugesan, P.N. Anantharamaiah, N. Manikanda Prabu, Fabrication of magnetically recoverable BiVO4/NiFe2O4 composites for the photocatalytic degradation of methylene blue, Ceram. Int. 47 (2021) 11526–11535, https://doi.org/10.1016/j.ceramint.2020.12.281.
[21] C. Ray, T. Pal, Recent advances of metal-metal oxide nanocomposites and their tailored nanostructures in numerous catalytic applications, J. Mater. Chem. A 5 (2017) 9465–9487, https://doi.org/10.1039/c7ta02116j.
[22] G. Seerangan Selvam, J. Sthevan Kovil Pitchai, K. Ammasai, T. Dheivasigamani, Performance analysis of three distinct NixV2Oy single-phase nano self-assemblies for asymmetric supercapacitor fabrication and effective detection of low-concentration hazardous herbicide, Dalt. Trans. 52 (2023) 14491–14509, https://doi.org/10.1039/d3dt02384b.
[23] R. Yu, N. Xue, S. Huo, J. Li, J. Wang, Structure characteristics and photoactivity of simultaneous luminescence and photocatalysis in CaV2O6 nanorods synthesized by the sol-gel Pechini method, RSC Adv. 5 (2015) 63502–63512, https://doi.org/10.1039/c5ra10465c.
[24] V.B. Taxak, Dayawati Sheetal, S.P. Khatkar, Synthesis, structural and optical properties of Eu3+-doped Ca2V2O7 nanophosphors, Curr. Appl. Phys. 13 (2013) 594–598, https://doi.org/10.1016/j.cap.2012.10.011.
[25] B. Shunmughananthan, T. Dheivasigamani, J. Sthevan Kovil Pitchai, S. Periyasamy, Performance comparison of distinct bismuth molybdate single phases for asymmetric supercapacitor applications, Dalt. Trans. 51 (2022) 15579–15592, https://doi.org/10.1039/d2dt02092k.
[26] A. Sharma, M. Varshney, K.H. Chae, S.O. Won, Electronic structure and luminescence assets in white-light emitting Ca2V2O7, Sr2V2O7 and Ba2V2O7 pyro-vanadates: X-ray absorption spectroscopy investigations, RSC Adv. 8 (2018) 26423–26431, https://doi.org/10.1039/c8ra03347a.
[27] S. Kumar, P.D. Sahare, Photocatalytic activity of bismuth vanadate for the degradation of organic compounds, Nano 8 (2013) 1–9, https://doi.org/10.1142/S1793292013500070.
[28] A. Pirvaram, E. Taheri-Nassaj, H. Taghipour-Armaki, W. Lu, W. Lei, H. Barzegar Bafrooei, Study on structure, microstructure and microwave dielectric characteristics of CaV2O6 and (Ca0.95M0.05)V2O6 (M=Zn, Ba) ceramics, J. Am. Ceram. Soc. 102 (2019) 5213–5222, https://doi.org/10.1111/jace.16370.
[29] M.S. Islam, H. Kabir, Y. Inagaki, A.R. Sarker, Comparative study of the conductivity of synthesized bivalent vanadates CaV2O6 and MnV2O6, J. Alloys Compd. 829 (2020) 154499, https://doi.org/10.1016/j.jallcom.2020.154499.
[30] H. Zhai, J. Qi, Y. Tan, L. Yang, H. Li, Y. Kang, H. Liu, J. Shang, H.S. Park, Construction of 1D-MoS2 nanorods/LiNb3O8 heterostructure for enhanced hydrogen evolution, Appl. Mater. Today 18 (2020) 100536, https://doi.org/10.1016/j.apmt.2019.100536.
[31] S. Zhang, W. Mu, Fabrication of Ca2V2O7 microspheres and its application in lithium-ion batteries, Mater. Lett. 183 (2016) 311–314, https://doi.org/10.1016/j.matlet.2016.07.131.
[32] S.X. Li, X.J. Liu, R.H. Mao, Z.R. Huang, R.J. Xie, Red-emission enhancement of the CaAlSiN3:Eu2+ phosphor by partial substitution for Ca3N2 by CaCO3 and excess calcium source addition, RSC Adv. 5 (2015) 76507–76515, https://doi.org/10.1039/c5ra14320a.
[33] I.M. Nagpure, M.M. Duvenhage, S.S. Pitale, O.M. Ntwaeaborwa, J.J. Terblans, H. C. Swart, Synthesis, thermal and spectroscopic characterization of Caq2 (calcium 8-hydroxyquinoline) organic phosphor, J. Fluoresc. 22 (2012) 1271–1279, https://doi.org/10.1007/s10895-012-1069-6.
[34] J. Forero-Saboya, C. Davoisne, R. Dedryvère, I. Yousef, P. Canepa, A. Ponrouch, Understanding the nature of the passivation layer enabling reversible calcium plating, Energy Environ. Sci. 13 (2020) 3423–3431, https://doi.org/10.1039/d0ee02347g.
[35] M. Minakshi, D.R.G. Mitchell, C. Baur, J. Chable, A.J. Barlow, M. Fichtner, A. Banerjee, S. Chakraborty, R. Ahuja, Phase evolution in calcium molybdate nanoparticles as a function of synthesis temperature and its electrochemical effect on energy storage, Nanoscale Adv. 1 (2019) 565–580, https://doi.org/10.1039/c8na00156a.
[36] R. Manikandan, C.J. Raj, M. Rajesh, B.C. Kim, J.Y. Sim, K.H. Yu, Electrochemical behaviour of lithium, sodium and potassium ion electrolytes in a Na0.33V2O5 symmetric pseudocapacitor with high performance and high cyclic stability, Chemelectrochem 5 (2018) 101–111, https://doi.org/10.1002/celc.201700923.
[37] H.T.T. Nguyen, D. Jung, C.Y. Park, D.J. Kang, Synthesis of single-crystalline sodium vanadate nanowires based on chemical solution deposition method, Mater. Chem. Phys. 165 (2015) 19–24, https://doi.org/10.1016/j.matchemphys.2015.05.053.
[38] S.A. Adewinbi, R.A. Busari, O.E. Adewumi, B.A. Taleatu, Effective photoabsorption of two-way spin-coated metal oxides interfacial layers: surface microstructural and optical studies, Surf. Interfaces 23 (2021) 101029, https://doi.org/10.1016/j.surfin.2021.101029.
[39] S. Liang, H. Wang, Y. Li, H. Qin, Z. Luo, B. Huang, X. Zhao, C. Zhao, L. Chen, Rare-earth based nanomaterials and their composites as electrode materials for high performance supercapacitors: a review, Sustain. Energy Fuels 4 (2020) 3825–3847, https://doi.org/10.1039/d0se00669f.
[40] R. Rahul, G. Seerangan Selvam, S. Moorthy Babu, A. Muthukaruppan, G. Bhoopathi, S. Nanthakumar, T. Dheivasigamani, Phase transition influenced photocatalytic dye degradation capability of pure and Eu-doped CoMoO4 polymorphic nanostructures, Phase Transitions 97 (2024) 484–499, https://doi.org/10.1080/01411594.2024.2348687.
[41] L. Zhang, X. Yuan, H. Wang, X. Chen, Z. Wu, Y. Liu, S. Gu, Q. Jiang, G. Zeng, Facile preparation of an Ag/AgVO3/BiOCl composite and its enhanced photocatalytic behavior for methylene blue degradation, RSC Adv. 5 (2015) 98184–98193, https://doi.org/10.1039/c5ra21453j.
[42] V.A. Online, M.M. Sajid, H. Zhai, N.A. Shad, A.M. Afzal, Y. Javed, S.B. Khan, N. Amin, Z. Zhang, RSC Adv. (2021) 13105–13118, https://doi.org/10.1039/d1ra00807b.
[43] M. Munir, N. Akthar, Y. Javed, S. Bashir, Preparation and characterization of Vanadium pentoxide (V 2 O 5) for photocatalytic degradation of monoazo and diazo dyes, Surf. Interfaces 19 (2020) 100502, https://doi.org/10.1016/j.surfin.2020.100502.
[44] E. Nyankson, B. Agyei-Tuffour, E. Annan, A. Yaya, B. Mensah, B. Onwona-Agyeman, R. Amedalor, B. Kwaku-Frimpong, J.K. Efavi, Ag2CO3-halloysite nanotubes composite with enhanced removal efficiency for water soluble dyes, Heliyon 5 (2019) e01969, https://doi.org/10.1016/j.heliyon.2019.e01969.
[45] V. Santhana, D. Thangaraju, A. Tanaka, W. Inami, S. JayaKumar, S. Matsuda, Development of hybrid TiO2/paint sludge extracted microbe composite for enhanced photocatalytic dye degradation, J. Inorg. Organomet. Polym. Mater. 30 (2020) 2805–2813, https://doi.org/10.1007/s10904-020-01448-2.